In search of an elusive Antarctic circumpolar wave in sea ice extents: 1978–1996

Per Gloersen & Norden E. Huang

For ease in discerning an Antarctic circumpolar wave in the perimeter of the ice pack, we construct a time series of the sea ice extents (essentially the area within the ice perimeter) in 1-degree longitudinal sectors for the period 1978–1996, as observed with the multichannel microwave imagers on board the NASA Nimbus 7 and the DOD (Dept. of Defense) DMSP (Defense Meteorological Satellite Program) F8, F11, and F13 satellites. After converting the time series into complex numbers by means of a Hilbert transform, we decompose the time series of the 360 sectors into its complex principal components (CPCs), effectively separating the spatial and temporal values. Then we decompose the real and imaginary parts of the temporal portions of the first three CPCs (complex principal compenents) by Empirical Mode Decomposition into their intrinsic modes, each representing a narrow frequency band, resulting in a collection of three CPCs for each intrinsic mode. Finally, we reconstruct the data in two different ways. First, we low-pass filter the data by combining all of the intrinsic modes of each CPC with periods longer than two years, which we designate as low-pass filtered. Next, we select the intrinsic mode of each CPC with periods of approximately four years, which we designate the quasiquadrennial (QQ) modes. The low-pass filtered time series shows eastward propagating azimuthal motion in the Ross and Weddell Seas, but no clearly circumpolar motion. The QQ time series, on the other hand, clearly shows eastward propagating circumpolar waves, but with occasional retrograde motion to the west.

P. Gloersen & N. E. Huang, Oceans and Ice Branch, Laboratory for Hydrospheric Processes NASA/Goddard Space Flight Center, Greenbelt, MD 20771, USA.

Introduction

Propagation of sea ice protuberances around Antarctica reported earlier by Cavalieri & Parkinson (1981) and more recently by White & Peterson (1996) and Parkinson (1998) are examined in this paper with a new analysis technique appropriate for non-stationary time series: an empirical decomposition into intrinsic mode functions (Huang et al. 1998). Previously, a spectral analysis (Gloersen & Mernicky 1998) was applied to the interior of the Antarctic sea ice pack using band-limited discreet Fourier transform of a shorter 1978–1987 sea ice time series. This provided phase distributions of two components observed in the ENSO signal, with periods of ca. 2.4 and 4.2 years, suggestive of a propagating wave in the interior of the pack. In this paper, we examine sea ice extents and employ a novel combination of Empirical Mode Decomposition (EMD) recently described by Huang et al. (1998) and Complex Singular Value Decomposition (CSVD). CSVD is used to separate the data into spatial and temporal components, and EMD is used to divide the temporal signal into distinct modes, representing narrow frequency pass-bands. Reconstruction of each intrinsic mode from its first three CPCs then permits construction of contour and three-dimensional plots that reveal the presence or absence of spatial propagation of its respective nodes.

Analysis

Here, for ease in discerning an Antarctic circumpolar wave in the perimeter of the ice pack, we construct a time series of the sea ice extents (the

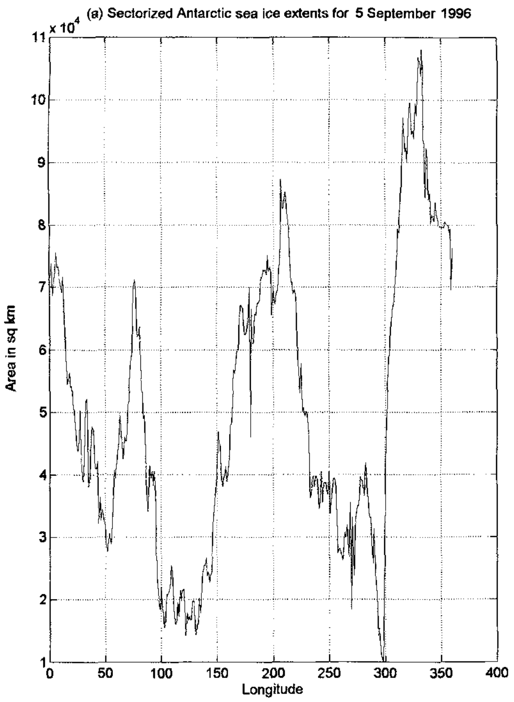

Fig. 1. Antarctic sea ice extents in 1° meridional sectors on 1 September 1996.

sum of the areas of pixels with ice concentrations of 15% or more) in 1-degree longitudinal sectors for the period 1978–1996, as observed with the multichannel microwave imagers on board the NASA Nimbus 7 and the DOD DMSP F8, F11, and F13 satellites. An example of the data is shown in Fig. 1 for a typical day in austral winter.

Next, Complex Singular Value Decomposition (CSVD) is used to decompose the time series of the 360 sectors into its principal components, after subtracting its linear trend line, effectively separating the spatial and temporal values. The results of the CSVD procedure can be expressed as:

$$\mathbf{Y}(3322,360) = \mathbf{U}(3322,360) * \mathbf{S}(360,360) * \mathbf{V}(360,360)' \tag{1}$$

where the original data have been subjected to a Hilbert transform to produce a complex data vector matrix, **Y**. **Y** is represented by the product of two complex unitary matrices, **U**, which contains the temporal information for each of the 360 CPCs and **V**, which contains the spatial information for each of the CPCs. **S** is a diagonal matrix of real eigenvalues. The prime on **V** denotes the matrix transpose. The number 3322 corresponds to the number of data days in the 18.2 year time series (including a 21 day data day gap in the DMSP F8 imager record), which has been interpolated with a modelled seasonal cycle (Gloersen, Campbell et al. 1992).

The spatial and temporal factors of the real part of the first three principal components are shown in Fig. 2. Plots of the eigenvalue ratios of the CPCs and also of the cumulative fraction of the signal in the first *n* modes (obtained by taking the ratio of the sum of the eigenvalues of the first *n* modes and the sum of all the eigenvalues) are shown in Figs. 3a and b. Fig. 3b indicates that about 34% of the signal is contained in the first three CPCs. Fig. 3a indicates that the amplitude of the fourth CPC is about 11% of the first. Thus, we need utilize only the first three CPCs to obtain a reasonable approximation to the original signal and to visualize any circumpolar wave that might be present.

The temporal portions of the first three CPCs are processed by means of Empirical Mode Decomposition (EMD) (Huang et al. 1998) into their intrinsic modes (IM), resulting in a collection of two or three CPCs for each intrinsic mode. It is important to note that the presence of several intrinsic modes for each CPC indicates that they are multi-modal. In particular, visual inspection of the temporal factor of CPC 1 (Fig. 2b) might lead one to conclude that it contains only the seasonal cycle but, as is shown later, this is far from the case. A simplistic description of this method of sifting a data vector, y(n), into nearly orthogonal intrinsic modes follows:

1. We obtain two vectors containing the extrema of y(n).
2. We fit the maxima and minima of these two vectors with cubic splines to produce two new vectors of length n.
3. We take the average of these two vectors to form a third new vector, $m_1(n)$.
4. The first intrinsic mode is then obtained by: $c_1 = y(n) - m_1(n)$.
5. We repeat steps 1–3 on $m_1(n)$ to obtain $m_2(n)$.
6. The second intrinsic mode is then obtained by: $c_2 = m_1(n) - m_2(n)$.

i. We imitate steps 5–6 (i–2) times until c_i contains less than one whole oscillation ($c_i = m_{i-1} - m_i$).

This process usually converges for i less than 11. The actual method is more complicated than this in that there are conditional tests for assuring that the

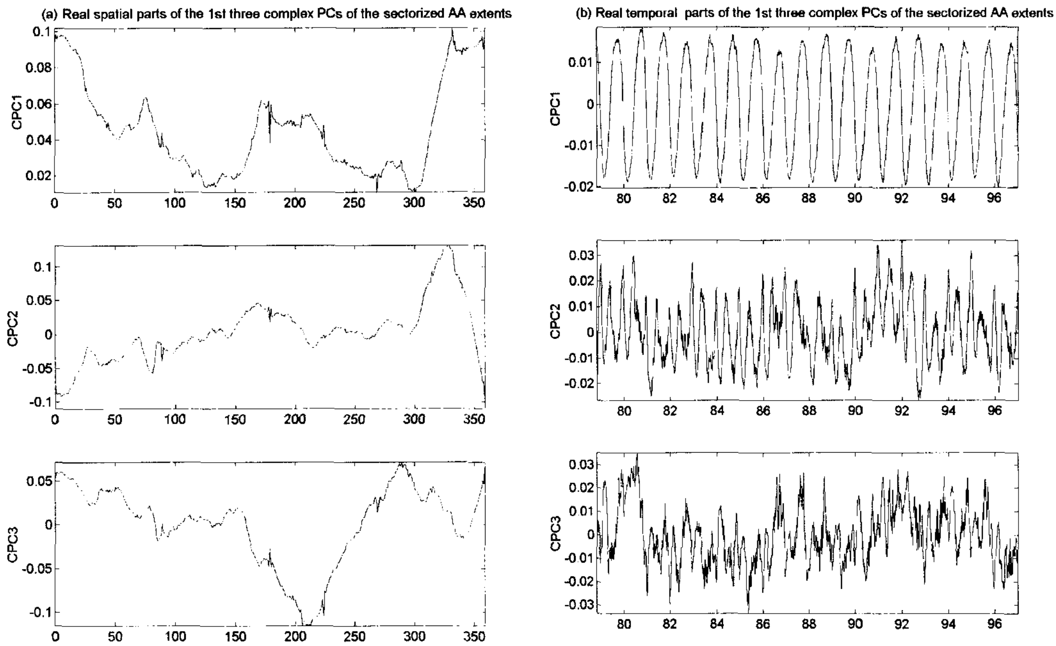

Fig. 2. Real parts of the first 3 Complex Principal Components of the time series of the Antarctic sea ice extents in 1° meridional sectors: (a) the spatial part; (b) the temporal part.

number of zero-crossings equals the number of extrema, for how many time series points are allowed between the extrema of the various modes, or how many are allowed between the extrema of the curvatures of the modes. If the input criteria are judiciously selected, the resultant modes are nearly orthogonal. A benefit of this approach is that the oscillations in the various modes are confined to narrow instantaneous frequency bands, greatly simplifying the interpretation of the results. Another benefit is that the original signal (within machine accuracy) is regained when the modes are added back together, an indication that spurious signals have not been introduced as a result of the decomposition.

The intrinsic modes of CPC1 are shown in Fig. 4. CPC1 appears to have 8 distinct oscillatory modes. The first mode contains the day-to-day fluctuations in the sea ice extent attributable to fluctuations in the weather. There is a flat area surrounded by two transients in this record occurring at the time of the aforementioned 21 day gap in the data, reflecting the lack of single day fluctuations in the interpolated data. The second mode is largely semi-monthly oscillations, possibly related to the 14 day tidal frequency. The third mode appears to be largely monthly oscillations, with an irregular amplitude modulation envelope of an annual cycle. We interpret these oscillations as influence of the monthly oceanic tides on the edge of the sea ice, and the minima of the envelope reflecting the reduction of signal when the ice is at its annual minimum extent. The fourth mode is a mixture of periods, of unknown origin, longer than one month and shorter than one year. The fifth mode is what we shall call the seasonal, rather than annual, cycle because it is not a monochromatic sinusoid. The shape of mode differs from the model seasonal cycle described earlier (Gloersen, Campbell et al. 1992) that consisted of the weighted sum of five harmonics of the annual cycle, and was found to approximate closely the observed seasonal cycles. The difference is attributable to the inability of Fourier analysis to produce a meaningful spectrum for a non-stationary phenomenon as discussed by Huang et al. (1998).

Modes 6–8 are of the most interest in the context of our search for a circumpolar wave in the Antarctic sea ice perimeter. Their amplitudes are, respectively, about 0.25, 0.1 and 0.05 of the seasonal cycle amplitude (Mode 5). Modes 6 and 7 are quasibiennial and quasiquadrennial periods similar to those observed earlier in the hemispheric

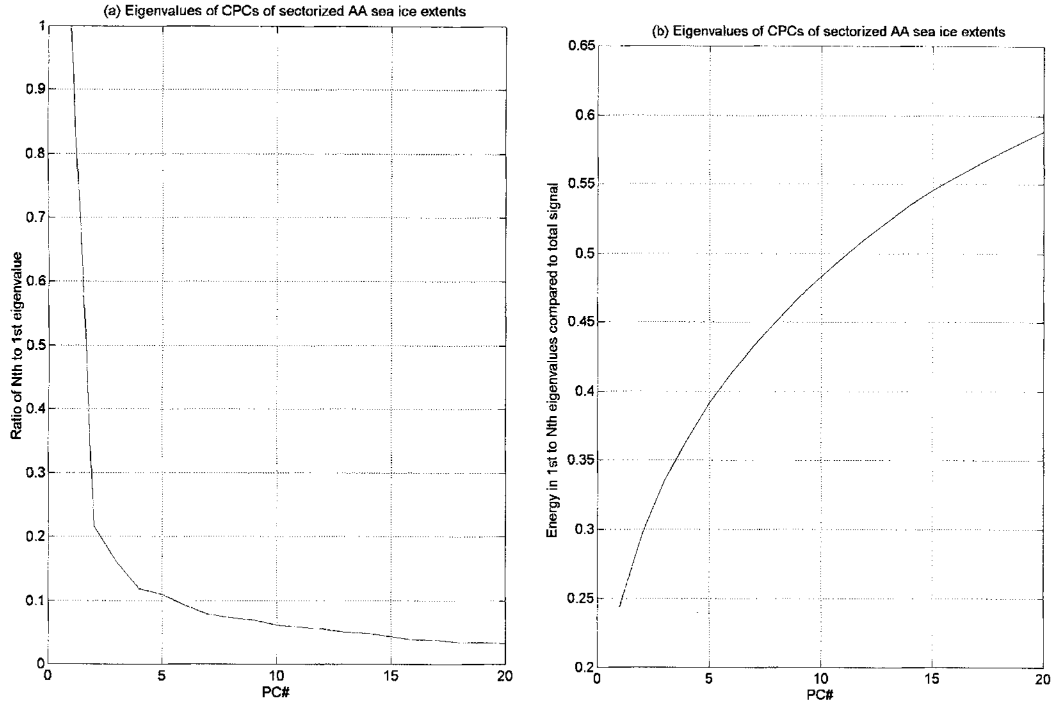

Fig. 3. (a) Eigenvalue ratios of the first 20 Complex Principal Components. (b) Percent of signal in the first N Principal Components, obtained from the ratio of the sum of the first N eigenvalues to their total sum.

sea ice canopies with band-limited Fourier analysis of a 9 year Nimbus 7 data record (Gloersen 1995; Gloersen, Yu et al. 1996; Gloersen & Mernicky 1998) which we attribute to an atmospheric or oceanic teleconnection with the El Niño and Southern Oscillation phenomena. Mode 8 contains periods in the range 6–7 years, and was only hinted at in the earlier studies of the 9 year data set (Gloersen 1995; Gloersen & Mernicky 1998). Finally, the last mode (9) contains the residual trend of the data set remaining after the initial subtraction of the trend line obtained by ordinary least squares. Although it displays some curvature, Mode 9 cannot be described convincingly as oscillatory.

The similarity between the modal structure of each of the first three CPCs and the rapid fall-off of their eigenvalues permit reconstruction of the original signal from its first three CPCs to a good approximation. Furthermore, the intrinsic modes of the original data can be reconstructed to a good approximation from the individual intrinsic modes of the first three CPCs.

We have reconstructed the data in two different ways. First, to simulate the 3–7 year bandpass filter used earlier by White & Peterson (1996), we have added together the intrinsic modes 7–9 of CPC1 (and similar modes of CPC2 and 3) to reconstruct a low-pass filtered time series. This excludes the quasibiennial modes (Mode 6 of CPC1) as well as the seasonal and shorter period modes. Second, we isolate the quasiquadrennial (QQ) mode (Mode 7 in CPC1) to look for differences between the QQ and low-pass filtered results.

Time/longitude contours of the low-pass filtered data (Fig. 5a) show eastward propagating azimuthal motion, but no complete circumpolar circuit. The most prominent one begins in about 1990, with the crest at about 220°E and the trough at about 320°E. The crest propagates eastward until about 1994, when it reaches about 40°E. The trough reaches 40°E in about 1992. The complicated combination of stationary and propagating troughs may be seen from a different perspective in the three-dimensional contour diagram in Fig.

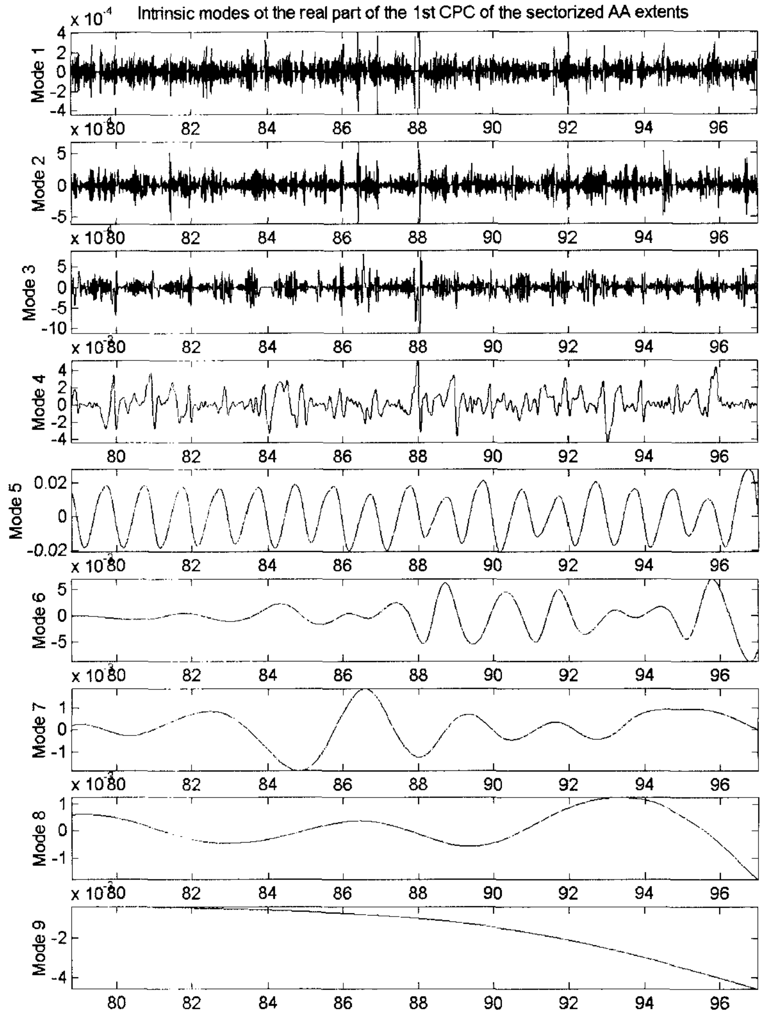

Fig. 4. Intrinsic modes of the real temporal part of the first Complex Principal Component.

5b. There seems to be a barrier between about 120–150°E (the part of the Southern Ocean south of the western Pacific) that the propagating waves do not cross.

The aforementioned barrier appears to be absent in the propagation patterns of the QQ modes shown in Fig. 6. Focusing again on two of the most prominent features, a trough beginning in about 1984 at about 220°E propagates eastward to 360°E until about mid-1986, then regresses westward for about half a year, resuming the eastward propagation to reach 360°E once again in about 1994, and finally stopping at about 20°E in about mid-1995. Thus, the trough propagated for about 1.5 circumpolar cycles at a rate of about 1 cycle in 8 years, as reported earlier (White & Petersen 1996; White, pers. comm.). The adjacent crest, starting at about 220°E, begins in about mid-1985. It propagates eastward, crossing the Greenwich Meridian in about 1985. There is a brief westward regression in about mid-1989, after which the crest continues eastward to about 300°E in about mid-1995 at which point the it begins another westward regression.

Discussion

White & Peterson (1996) have reported eastward propagation of a circumpolar wave in sea ice

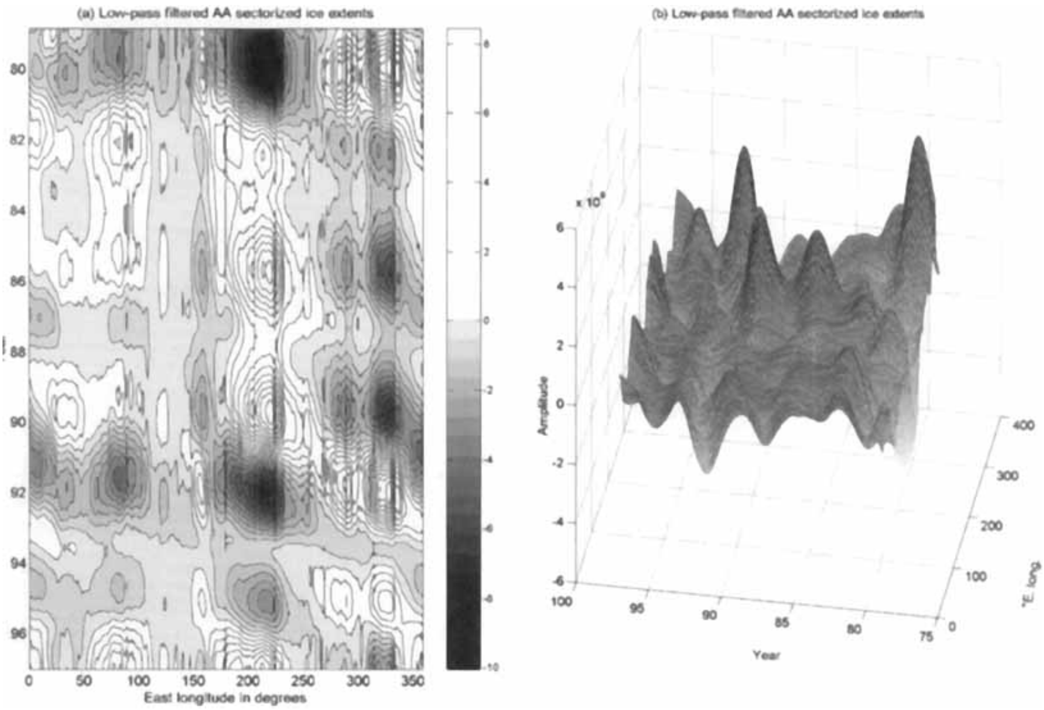

Fig. 5. (a) Contour plot of the low-pass filtered data of the sectored Antarctic sea ice extents reconstructed from the sum of the intrinsic modes with periods longer than three years of the first three Principal Components. Wave crests are white and troughs are shades of gray. (b) Three-dimensional plot of the data in (a).

extents, as well as in sea level pressures, and sea surface winds and temperatures. The data were preprocessed by passing through a band-pass filter with admittance from 3 to 7 years. They analysed sea ice extents in 5° meridional sectors, and the other parameters along the 56°S parallel. They interpreted the contour patterns on their resulting position-time diagrams as circumpolar waves propagating eastwards and completing the circular traverse in about a decade (White, pers. comm.). Thus the low-pass filter procedure we report here should encompass the entire oscillatory behaviour band-passed through their filter.

Our initial motive in undertaking this investigation was to confirm and examine in detail the circumpolar wave in sea ice extents reported by White & Peterson (1996). However, our sea ice extent results obtained with our low-pass filter do not agree with theirs. We surmise that their binning of the sea ice extents into 5° sectors, limiting the spatial resolution to about 10° of longitude, may have bridged the "barrier" between 120–150° that we observe in our low-pass filtered results. Alternatively, the high frequency end of their band-pass filter, a half-power point of three years, may suppress part of the signal admitted by our low-pass filter. Certainly, when we eliminate oscillations of three years or less with our QQ filter, our results are much more in agreement.

The results we present here clearly demonstrate the necessity of using a complex number representation of the time series in order to retain the circumpolar motion in the sea ice pack when applying singular value decomposition. Our earlier attempt at observing the circumpolar motion with real numbers was not successful. The results demonstrate also that care must be used in selecting the appropriate filters and the need for high spatial resolution in order not to lose important details in the wave propagation. Finally, we demonstrate that it is imprudent to presume that complex principal components in themselves represent fundamental modes of an oscillatory system. For instance, the first CPC shown here could easily be mistaken by inspection for the seasonal cycle. While it is true that the seasonal

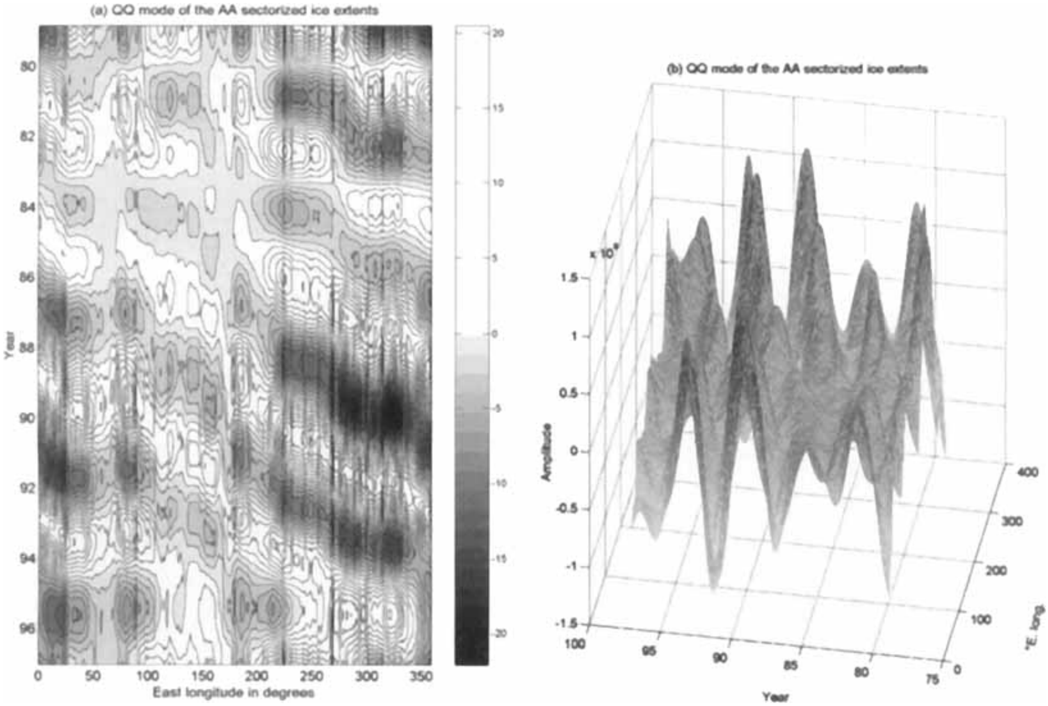

Fig. 6. (a) Contour plot of the intrinsic seasonal mode of the sectored Antarctic sea ice extents reconstructed from the quasiquadrennial (QQ) parts of the first three Principal Components. Wave crests are white and troughs are shades of gray. (b) Three-dimensional plot of the data in (a).

cycle is the largest oscillatory component of the first CPC, we have shown that the first CPC also has seven other significant oscillatory modes.

We intend to apply this technique also to the interior of the ice pack and to nearby sea surface temperatures and winds in an attempt to elucidate our present observations.

Acknowledgements. – This research was supported by the Office of Polar Programs, NASA Headquarters.

References

Cavalieri, D. J. & Parkinson, C. L. 1981: Large-scale variations in observed Antarctic sea ice extent and associated atmospheric circulation. *Monthly Weather Rev. 109*, 2323–2336.

Cavalieri, D. J., Gloersen, P., Parkinson, C. L., Comiso, J. C. & Zwally, H. J. 1997: Observed asymmetry in global sea ice changes. *Science 278*, 1104–1106.

Gloersen, P., Campbell, W. J., Cavalier, D. J., Comiso, J. C., Parkinson, C. L. & Zwally, H. J. 1992: Arctic and Antarctic sea ice, 1978–1987: satellite passive microwave observations and analysis. *NASA SP511*. 319 pp. Washington, D.C.: Government Printing Office.

Gloersen, P. 1995: Modulation of hemispheric sea ice covers by ENSO events. *Nature 373*, 503–508.

Gloersen, P., Yu, J. & Mollo-Christensen, E. 1996: Oscillatory behavior in Arctic sea ice concentrations. *J. Geophys. Res. 101*, 6641–6650.

Gloersen, P. & Mernicky, A. 1998: Oscillatory behavior in Antarctic sea ice concentrations. In M. O. Jeffries (ed.): *Antarctic sea ice: physical processes, interactions and variability. Antarct. Res. Ser. 74*, 161–171.

Huang, N. E., Shen, Z., Long, S. R., Wu, M. C., Shih, H. H., Zheng, Q., Yen, N.-C., Tung, C. C. & Liu, H. H. 1998: The Empirical Mode Decomposition and the Hilbert spectrum for nonlinear and nonstationary time series analysis. *Proc. R. S. Lond. Ser. A 454*, 903–995.

Parkinson, C. L. 1998: Length of the sea ice season in the Southern Ocean, 1988–1994. In M. O. Jeffries (ed.): *Antarctic sea ice: physical processes, interactions and variability. Antarct. Res. Ser. 74*, 173–186.

White, W. B. & Peterson, R. G. 1996: An Antarctic circumpolar wave in surface pressure, wind, temperature, and sea-ice extent. *Nature 380*, 699–702.